J Appl Electrochem (2007) 37:681–689
DOI 10.1007/s10800-007-9300-x

ORIGINAL PAPER

Inhibitors with biocidal functionalities to mitigate corrosion on mild steel in natural aqueous environment

D. Gopi · K. M. Govindaraju · S. Manimozhi · S. Ramesh · S. Rajeswari

Received: 12 September 2006 / Accepted: 25 January 2007 / Published online: 7 March 2007

Abstract The corrosion inhibition of mild steel by means of newly synthesised triazole phosphonates 3-Vanilidene amino 1,2,4-triazole phosphonate (VATP), 3-Anisalidene amino 1,2,4-triazole phosphonate (AATP) and 3-paranitro benzylidene amino 1,2,4-triazole phosphonate (PBATP) was studied along with cetyl trimethyl ammonium bromide (CTAB) in natural aqueous environment using weight loss measurement, potentiodynamic polarisation and ac impedance measurement. Surface characterisation techniques like FT-IR, XRD and EDXA were also carried out to understand the corrosion inhibition mechanism. Addition of molybdate increases the inhibition efficiency of triazole in a synergistic manner. Results from experimental observation have indicated VATP as a better corrosion inhibitor for mild steel in aqueous solution. Additionally the formulation consisting of VATP, sodium molybdate and CTAB offered good corrosion inhibition efficiency.

Keywords Biocide · Corrosion · Inhibitors · Mild steel · Phosphonate · Triazole

D. Gopi (✉) · K. M. Govindaraju · S. Manimozhi
Department of Chemistry, Periyar University, Salem 636 011 Tamil Nadu, India
e-mail: periyaruniversitygopi@yahoo.co.in

S. Ramesh · S. Rajeswari
Department of Analytical Chemistry, University of Madras, Chennai 600 025 Tamil Nadu, India

1 Introduction

The corrosion control of mild steel in neutral or slightly alkaline oxygen containing solutions is important for cooling water system operations. A study of mechanisms of the action of corrosion inhibitors has relevance both from the point of view of a search for new inhibitors and also for their effective application [1]. Most of the well-known inhibitors are organic compounds containing nitrogen, sulphur and oxygen atoms. Aromatic nitrogen salts are not only excellent inhibitors of iron dissolution, but also absorb hydrogen. It is well known that triazole types of organic compounds are good corrosion inhibitors for many metals and alloys in various aggressive media [2–8].

Fouling and corrosion are the two important operational problems in heat exchangers and associated cooling water system pipelines. The problems include flow blockage of pipes, pipe punctures and unacceptable general corrosion rates of the system components. For controlling fouling and corrosion in many industries the inhibitors are added continuously and biocides are added weekly once or once in a fortnight. Hence, it is essential to study the effect of inhibitors and biocides for cooling water system.

Phosphonic acids are noted for their hydrolytic stability, scale inhibiting property and ability to form complexes with metal cations. Thus they have been widely used as corrosion inhibitors [9–14]. Hence, in the present investigation some triazole derivatives containing the phosphonic acid group were synthesised and evaluated for their inhibition efficiency on mild steel in a neutral aqueous environment. In the present study 3-Vanilidene amino 1,2,4-triazole phosphonate (VATP), 3-Anisalidene amino 1,2,4-triazole

phosphonate (AATP) and 3-paranitro benzylidene amino 1,2,4-triazole phosphonate (PBATP) were used as inhibitors while biocide, Cetyl trimethyl ammonium bromide (CTAB) was used to study their effect on the corrosion process.

2 Experimental

2.1 Synthesis of triazole derivatives

All the tested azoles were synthesised in the laboratory as per the procedures detailed [15–17] and were characterised by their FT-IR and ^{1}H-NMR spectra. The structures of the compounds are given in Fig. 1.

2.2 Sample preparation

Mild steel specimens of following compositions were used for the experiment (wt%) C—0.13%, P—0.032%, Si—0.014%, S—0.025%, Mn—0.48% and Fe—balance. Prior to each experiment, the specimen was polished with SiC grit paper. Then the specimen was washed several times with distilled water, acetone and finally dried. The exposed specimen having thickness 0.2 cm with an area of 4×2 cm^2 was used for weight loss measurements and 1 cm^2 for polarisation and impedance studies. Lake water was used as the electrolyte and its analysis was: Total dissolved salts 738 ppm, Total alkalinity 201 ppm, Cl^- 170 ppm. pH 7.99–8.0 and iron 0.1 ppm.

Name	Abbreviation	Structure
3-Vanilidene amino 1,2,4-triazole phosphonate	VATP	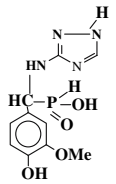
3-Anisalidene amino 1,2,4-triazole phosphonate	AATP	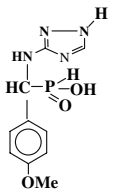
3-Para nitro benzylidene amino 1,2,4- triazole phosphonate	PBATP	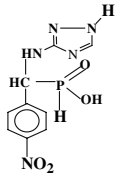

Fig. 1 Structure and name of the triazole derivatives

2.3 Weight loss experiments

The initial weight of the mild steel specimen before the corrosion test was noted. Mild steel specimens in triplicate were immersed in the test solution for a period of 3 days. The specimens were removed and cleaned according to ASTM G-81 and reweighed. The loss in weight was determined and the efficiencies were assessed in the following systems.

2.3.1 System I

The inhibition efficiency of synthesised inhibitors was evaluated. Similarly molybdate was used along with inhibitors to determine the corrosion rate of mild steel in lake water.

2.3.2 System II

The biocide efficiency was assessed using CTAB as a biocide.

2.3.3 System III

The influence of inhibitors along with biocide (CTAB) and the interference effect between them has been studied. Inhibitors and biocide were added simultaneously to study corrosion inhibition efficiencies.

2.3.4 System IV

Biocide was added first; after 24 h inhibitors were added to the same electrolyte and subsequently corrosion rates were calculated.

2.4 Potentiodynamic polarisation measurement

Potentiodynamic polarisation studies were carried out using a Vibrant Potentiostat/Galvanostat model No. VSM/CS/30 at a scan rate of 1 mV s^{-1} under static conditions. A platinum electrode and saturated calomel electrodes (SCE) were used as auxiliary and reference electrodes, respectively. All the experiments were carried out at constant temperature of 30 ± 2°C with natural lake water as electrolyte. Polarisation studies were carried out in lake water containing various concentrations of additives (systems I–IV).

2.5 Electrochemical impedance measurement

Ac impedance investigations were carried out using an EG&G PARC Potentiostat Model 6310 analyser with M 398 software at 30 ± 2°C. Electrochemical impedance spectroscopy was employed in the region of 10 kHz to 100 MHz with the perturbation amplitude of 10 mV.

2.6 Accelerated leaching studies (ICP-AES)

During the anodic polarisation, metal dissolution takes place, releasing a considerable amount of metal ion from the material. The concentration of metal ions in the test solution was determined after ageing for one hour at an impressed potential of –690 mV which corresponds to the open circuit potential (OCP) of blank. The analysis was carried out using Inductively Coupled argon Plasma-Atomic Emission Spectroscopy (ICP-AES)— Thermo Jarrel Ash-Atom Scan USA.

2.7 Surface examination study

The mild steel specimens were immersed in various test solutions for a period of 30 days. The specimens were then taken out and dried. The nature of the film formed on the metal surface was analysed by the various surface analytical techniques. The Fourier Transform Infrared Spectra (FT-IR) were recorded using a Perkin–Elmer 1600 FT-IR spectrophotometer. XRD patterns of the film formed on the metal surface were recorded using a computer controlled X-ray powder diffractometer, JEOL JDX 8030 with CuK_{α}(Ni-filtered) radiation (λ = 1.5418 Å) at a rating of 40 kV, 20 mA. The nature of the surface was analysed by energy dispersive X-ray analysis (EDXA).

3 Results and discussion

3.1 Weight loss data

3.1.1 Inhibitors on Corrosion (system I)

All the synthesised inhibitors were tested for six different concentrations and their corresponding weight loss data are presented in Table 1. The corrosion rate decreased considerably with increase in concentration of each inhibitor and reached the maximum value in the range of 3–5 ppm. The optimum concentration of inhibitor was evaluated based on the inhibition efficiency. It was calculated using the following equation.

Table 1 Corrosion rate of mild steel in lake water in presence and absence of VATP, AATP and PBATP for 3 days (system I) obtained by weight loss method

Inhibitor	Concentration (ppm)	Corrosion rate (mpy)	I.E (%)
Blank	–	13.45	–
VATP	2	5.85	56.50
	3	5.31	60.52
	4	4.77	64.53
	5	5.79	56.95
	6	6.81	49.36
	8	7.73	42.52
AATP	2	7.88	41.41
	3	5.76	57.17
	4	6.73	49.96
	5	7.28	45.88
	6	7.45	44.60
	8	7.99	40.59
PBATP	2	8.86	34.12
	3	8.79	34.64
	4	7.81	41.93
	5	7.29	45.79
	7	7.44	44.68
	10	9.98	25.79

$$\text{I.E (\%)} = \frac{\text{Uninhibited corrosion rate} - \text{Inhibited corrosion rate}}{\text{Uninhibited corrosion rate}} \times 100$$

The compounds VATP, AATP and PBATP have maximum of 64.53, 57.17 and 45.79% inhibition efficiencies, respectively.

The inhibition efficiency with the addition of molybdate at various concentration levels to the lake water was determined. An optimum concentration of 5 ppm gave a maximum inhibition efficiency of 50.40%. The corrosion rate of mild steel in lake water in the presence and absence of inhibitors along with molybdate are shown in Table 2. In the presence of molybdate along with the inhibitors the inhibition efficiency was increased. The improved inhibition efficiency in the presence of molybdate agreed with earlier work [18–20]. The maximum corrosion inhibition efficacy of VATP with molybdate was 68.47%.

3.1.2 Biocide on corrosion (system II)

In system II, the effect of CTAB on the corrosion control of mild steel in neutral aqueous solution was investigated. The reason for selecting CTAB as biocide is that CTAB is not only a typical cationic surfactant, which is commercially available, but also a quaternary ammonium salt with a long hydrocarbon chain, whose

Table 2 Corrosion rate of mild steel in lake water in presence and absence of inhibitors for 3 days (system I)

Inhibitor (ppm)	Corrosion rate (mpy)	I.E (%)
Blank	13.45	–
Mo (2)	7.74	42.44
Mo (4)	7.48	44.39
Mo (5)	6.67	50.40
Mo (8)	7.37	45.20
VATP (4) + Mo (5)	4.24	68.47
AATP (3) + Mo (5)	4.90	63.57
PBATP (5) + Mo (5)	6.64	50.63

homologues have been used extensively as biocides and inhibitors [21–24]. In particular it is reported that the halides are the most effective derivatives since they increase the inhibiting tendency of the positive quaternary ammonium ions through a synergistic effect [21].

Table 3 shows the influence of CTAB on corrosion rate of mild steel in natural aqueous environment. The corrosion rate was found to decrease with increasing concentration up to 15 ppm, after which there was an increase. The tested biocide showed a maximum corrosion inhibition of 52.93%.

In the case of CTAB, the bromide ions were first chemisorbed on the metal surface, replacing the OH^- ions, and the positive cationic part of the cetyl group was held by physical (electrostatic) adsorption. This type of chemisorption can block the active sites vulnerable for corrosion and thus reduces corrosion [25].

3.1.3 Inhibitors and biocide on corrosion (system III and system IV)

In system III, inhibitors (VATP, AATP and PBATP) with molybdate and biocide were added at the same time and corrosion efficiency was calculated and is listed in Table 4. In the presence of CTAB with inhibitors AATP and PBATP, the efficiency was about 80.52% and 67.36%, respectively. Maximum inhibition efficiency of 82% was exhibited by VATP. At a given concentration of the inhibitor, the values for the degree

Table 3 Corrosion rate of mild steel in lake water in presence of biocide for three days (System II)

Biocide	Concentration (ppm)	Corrosion rate (mpy)	I.E (%)
Blank	–	13.45	–
CTAB	10	7.80	42.00
	15	6.33	52.93
	20	8.16	39.33
	30	8.65	35.68

Table 4 Corrosion rate of mild steel in lake water in presence of inhibitors and biocide for 3 days (system III and system IV)

Inhibitors	System	Conc. of inhibitor (ppm)	Corrosion rate (mpy)	I.E (%)
Blank	–	–	13.45	–
VATP + Mo + CTAB	System III	4 + 5 + 15	2.42	82.00
AATP + Mo + CTAB		3 + 5 + 15	2.62	80.52
PBATP + Mo + CTAB		5 + 5 + 15	4.39	67.36
CTAB + VATP + Mo	System IV	15 + 4 + 5	2.63	80.44
CTAB + AATP + Mo		15 + 3 + 5	3.17	76.43
CTAB + PBATP + Mo		15 + 5 + 5	4.88	63.71

of corrosion inhibition by the inhibitors are in the order VATP > AATP > PBATP.

As mentioned earlier in system IV, the CTAB was added first and after 24 h inhibitors were added. The corrosion inhibition efficacy of all the inhibitors with biocide in system IV for mild steel was calculated and is shown in Table 4. The corrosion inhibition was about 80.44% for VATP, while adding AATP and PBATP gave inhibition efficiencies of about 76.43% and 63.71%, respectively.

3.2 Potentiodynamic polarisation measurements

Potentiodynamic polarisation parameters of mild steel immersed in lake water for all four systems are given in Tables 5 and 6 and their corresponding polarisation curves are also shown in Figs. 2, 3, 4. The corrosion current of mild steel in the presence of inhibitor was much smaller than that in the absence of inhibitor. In the presence of inhibitors the corrosion potential slightly shifted in the cathodic direction in comparison to the result obtained in the absence of inhibitor. Both the anodic and cathodic current densities decreased indicating that all the inhibitors suppressed both the anodic and cathodic reactions, although mainly the cathodic one, which indicates predominantly cathodic

Table 5 Potentiodynamic polarisation parameters of mild steel in lake water with and without the inhibitor

Inhibitors (ppm)	OCP (mV vs. SCE)	E_{corr} (mV)	I_{corr} (mA cm^{-2})	I.E (%)
Blank	–690	–695	0.0325	–
VATP (4)	–761	–778	0.0043	86.76
AATP (3)	–756	–810	0.0048	85.23
PBATP (5)	–740	–750	0.0140	56.92
VATP (4) + Mo (5)	–750	–735	0.0035	89.23
AATP (3) + Mo (5)	–510	–804	0.0045	86.15
PBATP (5) + Mo (5)	–620	–720	0.0120	63.07

Table 6 Potentiodynamic polarisation parameters of mild steel in lake water. Mixing of biocide + inhibitor (System III and IV)

Inhibitors	OCP (mV vs. SCE)	E_{corr} (mV)	I_{corr} (mA cm^{-2})	I.E (%)
Blank	–690	–695	0.0325	–
VATP	–750	–650	0.0017	94.76
AATP	–665	–654	0.0021	93.53
PBATP	–515	–700	0.0100	69.23
Inhibitor addition after killing bacteria by addition of biocide (System IV)				
VATP	–720	–666	0.0025	92.30
AATP	–700	–682	0.0028	91.38
PBATP	–660	–712	0.0107	67.07

control. The percentage inhibition efficiencies for the various inhibitors and biocide were calculated using the formula

$$\text{I.E}\ (\%) = \frac{\left(i_{corr} - i'_{corr}\right)}{i_{corr}} \times 100$$

where, i_{corr} and i'_{corr} are the corrosion current in the absence and presence of inhibitors. A maximum inhibition efficiency of 86.76% was observed for VATP.

Addition of molybdate controls both the cathodic and anodic reaction. But along with inhibitor they also predominantly control the cathodic reaction sites. In the presence of molybdate, VATP shows a higher efficiency of 89.23% than VATP alone (86.76%). Many authors [26, 27] have studied the synergistic effect of molybdate with tolyl triazole (TTA). The synergism results in enhanced inhibition, which may be related either to interaction between the inhibitor compounds or to interaction between the inhibitor

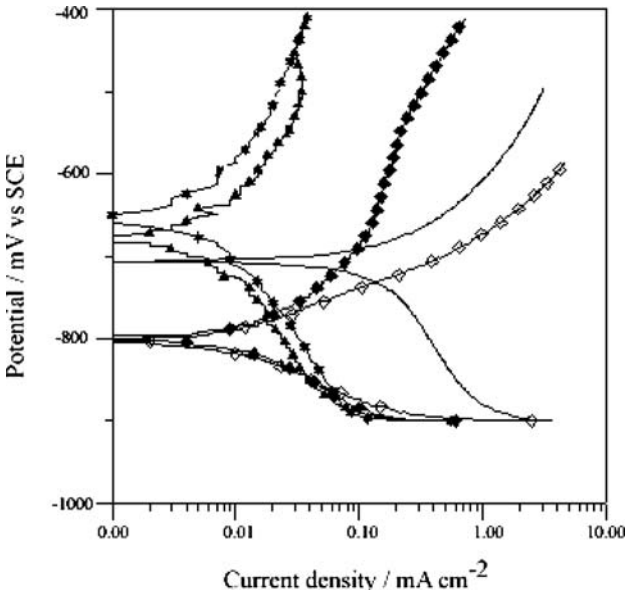

Fig. 3 Potentiodynamic polarisation curves of mild steel in lake water with and without AATP and biocide (—— Blank, —◇— AATP, —◆— AATP + Mo, —✸— System III of AATP and —▲— System IV of AATP)

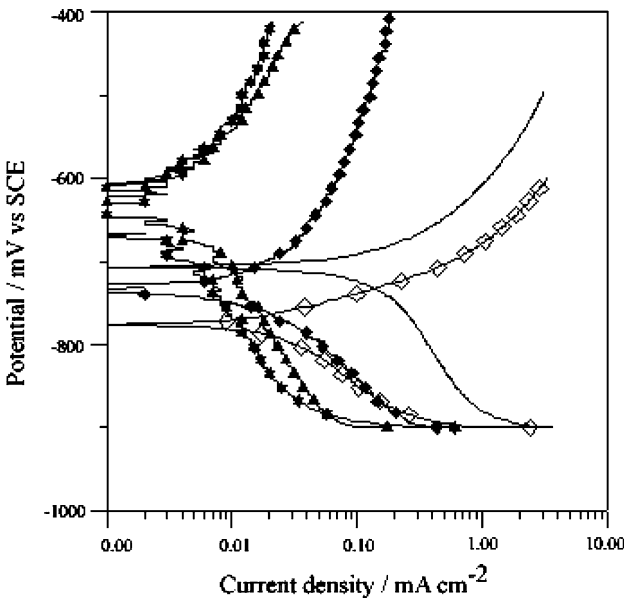

Fig. 2 Potentiodynamic polarisation curves of mild steel in lake water with and without VATP and biocide (—— Blank, —◇— VATP, —◆— VATP + Mo, —✸— System III of VATP and —▲— System IV of VATP)

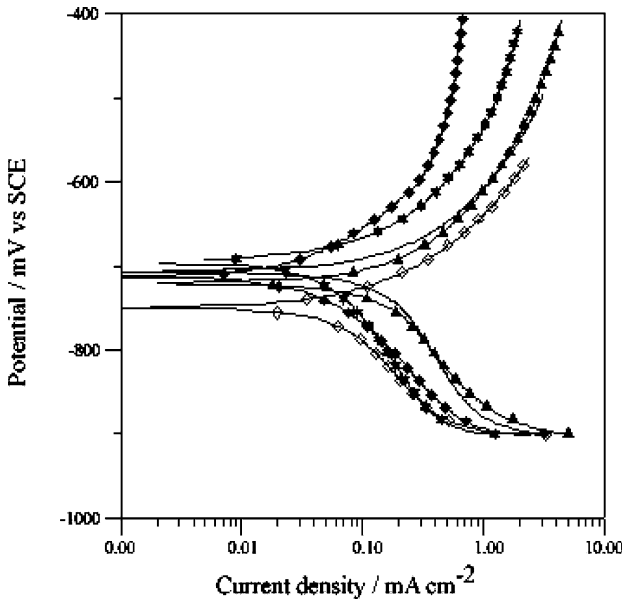

Fig. 4 Potentiodynamic polarisation curves of mild steel in lake water with and without PBATP and biocide (—— Blank, —◇— PBATP, —◆— PBATP + Mo, —✸— System III of PBATP and —▲— System IV of PBATP)

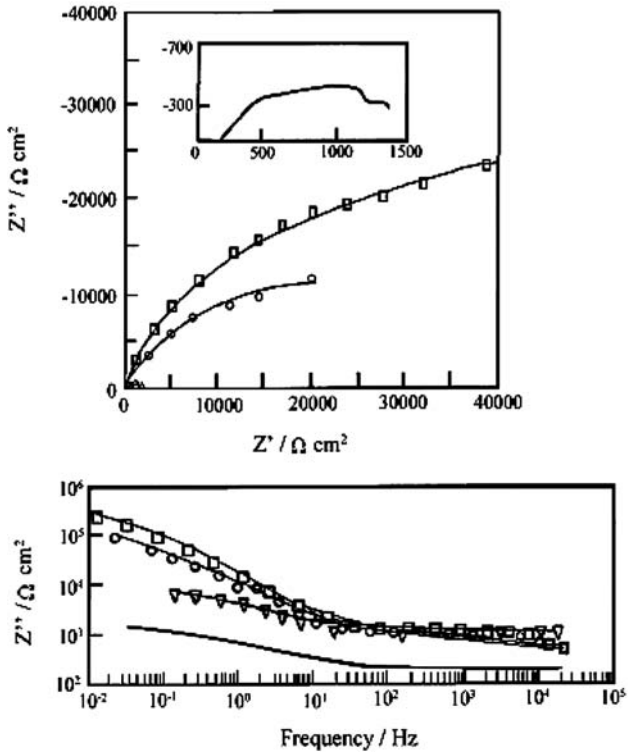

Fig. 5 Nyquist and Bode plot of mild steel in lake water with optimum concentration of VATP with biocide mixture (system III) (— Blank, □ VATP, ○ AATP and ∇ PBATP)

compound and one of the ions present in the aqueous medium.

In system III, a decrease in both the anodic and cathodic current densities implies that the inhibitors suppress both the anodic and cathodic reactions. In system III, the inhibition efficiency was about 94.76%, 93.53% and 69.23%, respectively for VATP, AATP and PBATP.

In system IV, the corrosion inhibition efficiency was lower compared to system III and the results are shown in Table 5 and 6. In the presence of AATP the efficiency was about 91.38% and OCP was –700 mV. The inhibition efficiency of VATP and PBATP (system IV) was about 92.30% and 67.07%, respectively. The combination of inhibitors with molybdate and biocide affords enhanced inhibition. In system III, the inhibitor recorded higher efficiencies than in system IV, which indicates an interaction between the biocide and the inhibitor system. This corroborates the results of the weight loss tests.

The higher inhibition efficiency of VATP may be attributed to the increased electron density leading to electron transfer from functional groups to the metal surface, producing greater coordinate bonding with a greater adsorption and inhibitor efficiency. A similar explanation has been proposed elsewhere [28, 29].

3.3 Electrochemical impedance measurements (EIS)

The admittance plots of mild steel in natural aqueous environment in the absence and presence of inhibitors and biocide are shown in Fig. 5. As the admittance plots were not semicircles these were not used for calculating the impedance parameters. The electrochemical parameters like solution resistance (R_s) and charge transfer resistance (R_{ct}) and double layer capacitance (C_{dl}) were obtained by using the semicircle fitting method [30]. This can be achieved by selecting the best fit for the semi circle on the complex plane (Nyquist) plot. The data were plotted and analysed using the software Z view version 1.5b, (1996, Scribner Associates Inc.).

Nyquist and Bode plots of mild steel in inhibited and uninhibited neutral aqueous solution containing various triazole phosphonates with biocide (system III) are shown in Fig. 5. The charge transfer resistance increased with the inhibitor biocide mixture and became ~2 times higher than for the blank value.

The increase in resistance and the decrease in double layer capacitance have been attributed to the enhanced adsorption of inhibitor molecules on the metal surface [31]. Increase in charge transfer resistance resulted in a decrease in metal dissolution. The EIS parameters like charge transfer resistance and capacitance with inhibitors were calculated and these are presented in Table 7. VATP exhibits the highest inhibition efficiency of 98.02%. The efficiencies calculated from ac measurements show the same trend as those observed from weight loss measurements and dc polarisation.

The low value of C_{dl} indicates thickening of the inhibitor film on the metal surface in the presence of both inhibitor and biocide. A high R_{ct} value corresponds to a high corrosion protection effect. This can be attributed to the formation of metal ion/inhibitor complexes.

Table 7 Electrochemical impedance parameters of mild steel immersed in lake water with optimum concentration of inhibitors and biocide (system III)

Compounds	R_{ct} (Ω cm^{-2})	C_{dl} (10^{-4}/F cm^{-2})
Blank	1414.12	2.54494
VATP	71561.2	0.70896
AATP	36716.4	1.13497
PBATP	2708.52	4.6629

Table 8 Concentration of iron present in the solution after leaching of mild steel at various inhibitor mixtures

Inhibitors	Concentration of metal ion (ppm)
Blank	7.2
VATP	0.3
AATP	0.4
PBATP	1.4

3.4 Accelerated leaching studies (ICP-AES)

The results of the accelerated leaching study are presented in Table 8, which shows the concentration of iron leached from the mild steel at an impressed potential of OCP (–690 mV). For mild steel significant amounts of iron were released into the solution even in the OCP region. Inhibitors with biocide mixtures exhibited leaching characteristics but the concentrations of metal ion leached out were low compared to blank.

In the present investigation VATP and AATP mixture exhibited a minimal leach of metal ion compared to blank. This can be attributed mainly to the stable complex film that inhibits metal dissolution by forming a barrier layer between the metal and the environment, thus preventing the bare metal contacting solution.

3.5 Surface evaluation studies

3.5.1 Analysis of FT-IR spectra

The FT-IR spectrum of VATP is presented in Fig. 6a. The FT-IR spectrum of the film formed on mild steel immersed in lake water with 4 ppm of VATP (Fig. 6c) reveals that the P^{+}–O^{-} stretching frequency of VATP has shifted from 1,080 cm^{-1} to 1,019 cm^{-1} [32, 33]. This indicates that the N and O atoms are coordinated with Fe^{2+}. The spectrum of the film formed in VATP with biocide (Fig. 6d) shows that the band at 930 cm^{-1} almost disappears and the P–O stretching frequency decreases from 1,080 cm^{-1} to 1,008 cm^{-1}. This suggests that the oxygen atom is coordinated to Fe^{2+} resulting in the formation of a Fe^{2+}–phosphonate complex on the metal surface.

The FT-IR spectrum of pure CTAB is shown in Fig. 6b. The absorption band at 2,854 cm^{-1} represents the CH_2 stretching frequency. The aliphatic C–H stretches cause absorption at 2,923 cm^{-1} and 2,854 cm^{-1}. The band at 1,126 cm^{-1} corresponds to C–N stretching. The absorption bands at 2,923 cm^{-1} and 2,854 cm^{-1} suggest the adsorption of CTAB on anodic sites. Since there is no shift in the absorption frequencies, CTAB has been adsorbed on the metal surface and the characteristic peaks corresponding to CTAB are obtained. From the results the CTAB provides an effective impervious barrier to the dissolution of metal and thus affords inhibition characteristics.

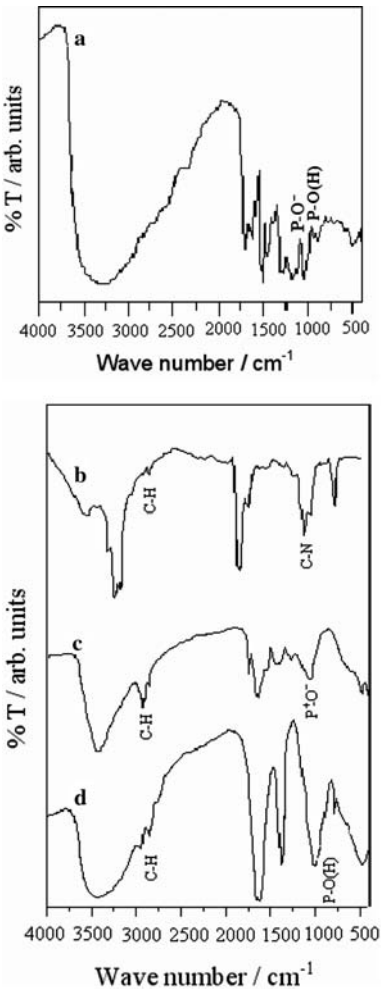

Fig. 6 Infrared transmission spectra of (a) VATP (b) CTAB Infrared reflection absorption spectrum of the film formed on the mild steel substrate after immersion in the solution containing (c) VATP (d) mixture of VATP + Mo + CTAB

Nitrogen containing organic heterocyclic compounds are excellent complex or chelate forming substances with transition metals [34]. Such complexes are strongly adsorbed, forming a thin, adherent film and providing a barrier between the metal surface and the corrosive medium.

The formation of a complex is the result of reaction between the triazole on the metal surface through the NH group and the metal cation formed during corrosion. It is known that aromatic triazoles are effective

inhibitors for iron and its alloys [35]. The protective action of the triazole is based on the formation of a semi-permeable, insoluble, polymeric copper–triazole complex film. The polymeric complex is formed by covalent and coordinate covalent bonds.

The adsorption (chemisorption) may be viewed as a result of Lewis acid–base electron exchange, resulting in the formation of 5- and 6-membered metal inhibitor ring complexes (except O–PO_4, which forms a 4-membered ring), as shown in Fig. 7 [36]. These metal inhibitor complexes successfully inhibit corrosion if they have a large surface activity and a low level of aqueous solubility.

3.5.2 X-ray diffraction (XRD) Analysis

The XRD pattern of the mild steel immersed in the blank and the solution containing 4 ppm VATP + 5 ppm Mo + 15 ppm CTAB is shown in Fig. 8. The peaks due to oxides of iron such as Fe_3O_4 and Γ-FeOOH are absent and those due to iron alone are observed at $2\theta = 43.6$, 50.7 and 74.3°. It can be inferred that oxides of iron such as FeOOH and Fe_3O_4 are absent from the metal surface (Fig. 8b).

3.5.3 Energy dispersive X-ray analysis (EDXA)

Examination of the mild steel surface after exposure to lake water with and without inhibitor and biocide was carried using EDXA. In order to define more accurately the nature of the corrosion layers, elemental mapping of Fe, P and S was carried out by EDXA. Phophorus and iron were prominent in the spectrum (Fig. 9). The phosphorus peak was due to the fact that the lake water was treated with a phosphonate-based inhibitor. The distribution of the elements was non-homogeneous, showing a thin layer at the surface.

The EDXA spectra showed several peaks for elements such as calcium, iron and silicon, but the strongest peaks were for iron and phosphorus. This suggests that the layer was composed of iron in addition to phosphorus, silicon and other minor constituents. The instrument used was not capable of detecting oxygen and sodium.

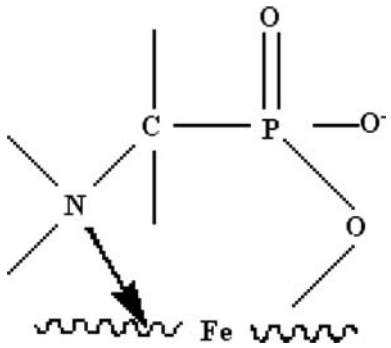

Fig. 7 Fe–phosphonate complex

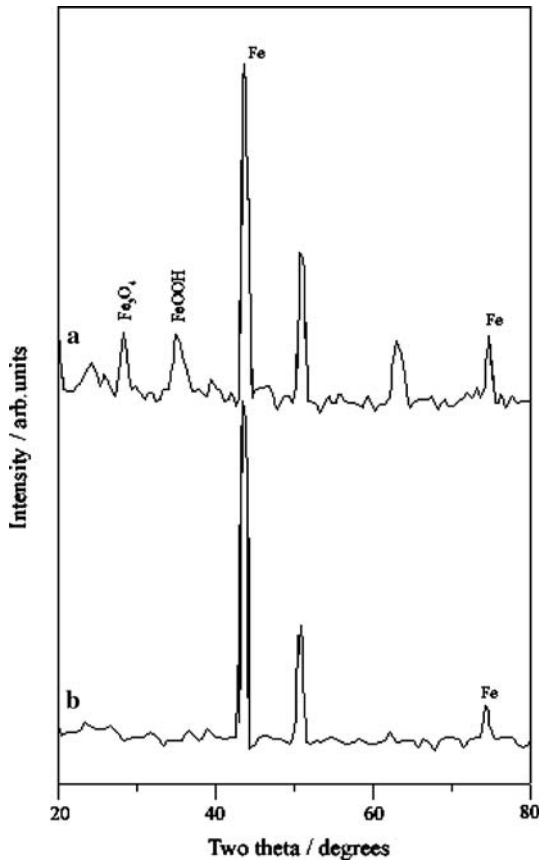

Fig. 8 XRD pattern obtained on the surface film formed on mild steel at the end of 30 days in different environment. Curve: (**a**) Blank, (**b**) VATP + Mo + CTAB

4 Conclusion

All the inhibitors act as cathodic inhibitors. The inhibition efficiency follows the order VATP > AATP > PBATP. The weight loss and polarisation measurements indicate that the simultaneous addition of inhibitors and biocide (system III) show a greater efficiency than in system IV. A high R_{ct} and low C_{dl} value indicates a high protection effect in the presence of inhibitors and biocide. From the corrosion point of view, VATP and AATP with Mo act as a good inhibitor system. The formulation consisting of 4 ppm of VATP, 5 ppm of Mo and 15 ppm of CTAB has 95% corrosion inhibition efficiency. A similar formulation for 4 ppm of AATP along with Mo and CTAB (5 ppm and 15 ppm) has 92% corrosion inhibition efficiency.

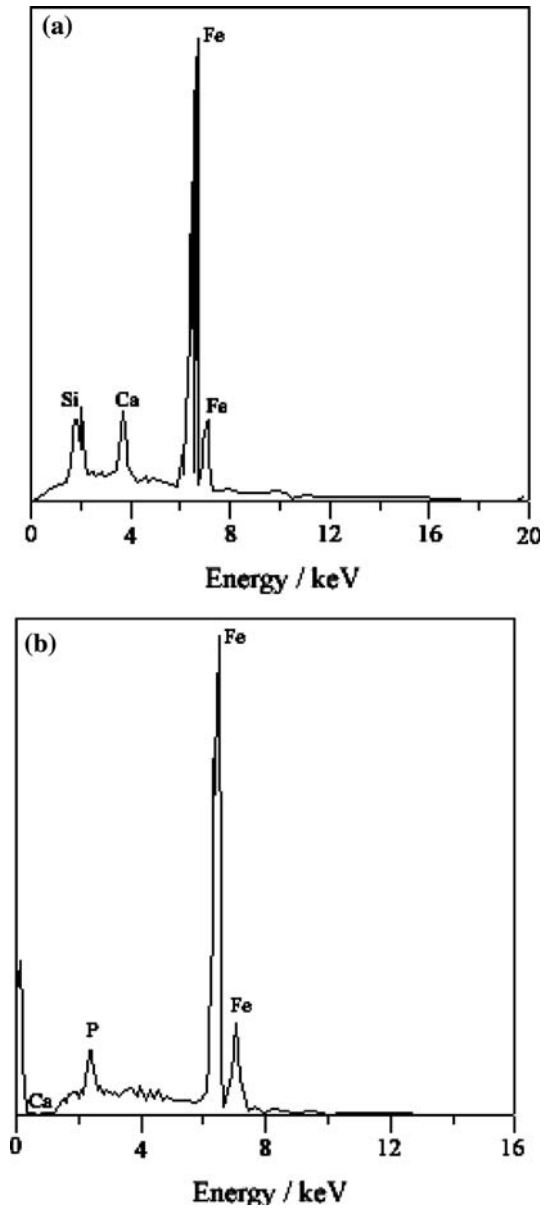

Fig. 9 EDXA spectrum of mild steel in natural lake water (**a**) Blank (**b**) VATP with biocide mixture

Corrosion inhibition is probably due to the formation of a protective film consisting of a Fe–phosphonate complex.

References

1. Trabanelli G (1991) Corrosion, 47:410
2. Tadros AB, Abdenaby BA (1988) J Electroanal Chem 246:433
3. Agrawal R, Namboodhiri TKG (1992) J Appl Electrochem 22:383
4. Mernari B, Elattari H, Traisnel M, Bentiss E, Largrenee M (1998) Corros Sci 40:391
5. Bentiss E, Lagrenee M, Traisnel M, Hornez JC (1999) Corros Sci 41:789
6. Ramesh S, Rajeswari S (2004) Electrochim Acta 49:811
7. Wang L (2006) Corros Sci 48:608
8. Elmehdi B, Mernari B, Traisnel M, Bentiss F, Lagrenee M (2003) Mater Chem Phys 77:489
9. Serkine I, Kirakawa Y (1986) Corrosion 42:276
10. Horvath T, Kalman E, Kutsan G, Rausher A (1994) Brit Corros J 29:215
11. Fang JL, Li Y, Ye XR, Wang ZW, Liu Q (1993) Corrosion 49:266
12. Ramesh S, Rajeswari S (2005) Corros Sci 47:151
13. Ramesh S, Rajeswari S, Maruthamuthu S (2004) Appl Surf Sci 229:214
14. Gunasekaran G, Natarajan R, Palaniswamy N (2001) Corros Sci 43:1615
15. Ramesh S, Rajeswari S, Maruthamuthu S (2002) Proceedings of national convention on corrosion (CORCON-2002), East Asia Pacific Regional conference, Goa, India (2002)
16. Shaban A, Kalman E, Biczo I (1993) Corros Sci 35:1463
17. Ramesh S, Rajeswari S (2003) Can Metall Quart 42:377
18. Stranick MA (1984) Corrosion 40:296
19. Mu G, Li X, Qu Q, Zhou J (2006) Corros Sci 48:445
20. Alentejano CR, Aoki IV (2004) Electorchim Acta 49:2779
21. Schwesberg DP, Ashworth V (1988) Corros Sci 28:639
22. Ma H, Chen S, Zhao S, Liu X, Li D (2001) J Electrochem Soc 148:B482
23. Lalitha A, Ramesh S, Rajeswari S (2005) Electrochim Acta 51:47
24. Qiu L-G, Xie A-J, Shen Y-H (2005) Mater Chem Phys 91:269
25. Ma H, Chen S, Yin B, Zhao S, Liu X (2003) Corros Sci 45:867
26. Veres A, Reinhard G, Kalman E (1992) Brit Corros J 27:147
27. Vukasovich MS (1990) Mater Perform 29:48
28. Khamis E, Atea M (1994) Corrosion 50:106
29. Fouda AS, Moussa MN, Taha FI, El-Neamaa AI (1986) Corros Sci 26:719
30. Basia of A.C. Impedance measurements, Application note-AC-1, Egand G. Princeton Applied Research, Electrochemical Instrument Division, Princeton, NJ (1982)
31. Lagrenee M, Mernari B, Bouanis M, Traisnel M, Bentiss F (2002) Corros Sci 44:573
32. Cross AD (1990) Introduction to practical infrared spectroscopy. Butterworths Scientific Publication, London, p 73
33. Kazuo Nakamoto (1986) Infrared and raman spectra of inorganic and coordination compounds. Willey Interscience, New York, p 168
34. Patel NK (1972) J Electrochem Soc India 21:136
35. Wu YC, Zhang P, Pickering HW, Allara DL (1993) J Electrochem Soc 140:2791
36. Saha G, Kurmaih N (1986) Corrosion 42:233